NANO EXPRESS　　　　　　　　　　　　　　　　　　　　　　　　　**Open Access**

Highly selective colorimetric detection and preconcentration of Bi(III) ions by dithizone complexes anchored onto mesoporous TiO$_2$

Mohd Faisal[1], Adel A Ismail[1,2*], Farid A Harraz[1,2], Houcine Bouzid[1,4], Saleh A Al-Sayari[1,3] and Ali Al-Hajry[1,4]

Abstract

We successfully developed a single-step detection and removal unit for Bi(III) ions based on dithizone (DZ) anchored on mesoporous TiO$_2$ with rapid colorometric response and high selectivity for the first time. [(DZ)$_3$-Bi] complex is easily separated and collected by mesoporous TiO$_2$ as adsorbent and preconcentrator without any color change of the produced complex onto the surface of mesoporous TiO$_2$ (TiO$_2$-[(DZ)$_3$-Bi]) at different Bi(III) concentrations. This is because highly potent mesoporous TiO$_2$ architecture provides proficient channeling or movement of Bi(III) ions for efficient binding of metal ion, and the simultaneous excellent adsorbing nature of mesoporous TiO$_2$ provides an extra plane for the removal of metal ions.

Keywords: Mesoporous TiO$_2$; Optical sensor; Detection; Preconcentration; Bi(III) ions

Background

Bi(III) ion in the environment is highly fatal to human beings and in particular to aquatic species in seawater. The development of solely selective, separation, preconcentration, and detection method for Bi(III) ions at ultratraces is a challenging task because of their very low concentrations in natural samples and strong interference from the real sample matrices. Thus, in recent years, considerable attention has been focused on the preconcentration and/or monitoring of ultratrace Bi(III) ions [1]. Solid phase extraction techniques have provided excellent alternative approach to liquid-liquid extraction for Bi(III) preconcentration prior to analyte determination step [2-4]. Several supporters such as silica [5-7], clays [8], biomass [9], resins [10,11], and carbons [12,13] have been modified with chelating groups for the adsorption of heavy metal ions. In our previous work, first molecular receptors were anchored onto mesoporous silica and then this framework was used for the

detection of metal ions [14-21]. However, few reports are available for the detection of heavy metals using TiO$_2$ films [22,23]. Nanocrystalline TiO$_2$ films were employed for naked-eye colorimetric detection of mercury in aqueous solution using N719 dye (N719 = *bis*(2,2A-bipyridyl-4,4A-dicarboxylato) ruthenium(II) *bis* (tetrabutylammonium) *bis*(thiocyanate)) [22,23]. Mesoporous TiO$_2$ is supposed to be a potentially active material for designing optical sensor due to its excellent surface area and high optical transparency in the visible part of the spectrum [22]. When mesoporous TiO$_2$ is dispersed in water, then the surface becomes anionic in nature and increases in surface area that would render the more coverage of hydroxyl groups (OH) from H$_2$O [24]. In sensing application, mesoporosity provides the desired high accessible surface and easier movement of metal ions for efficient binding; simultaneously excellent adsorbing properties of mesoporous TiO$_2$ provide an extra plane for removal of metal ion. In this contribution, we successfully detect and preconcentrate Bi(III) ion in a single step using mesoporous TiO$_2$ without any color change of the produced complex [(DZ)$_3$-Bi] onto the surface of mesoporous TiO$_2$ {TiO$_2$-[(DZ)$_3$-Bi]} at different Bi(III) concentrations. To the best of our knowledge, this is the first report briefing the single-step

* Correspondence: adelali141@yahoo.com
[1]Promising Centre for Sensors and Electronic Devices (PCSED), Advanced Materials and Nano-Research Centre, Najran University, P.O. Box 1988, Najran 11001, Saudi Arabia
[2]Nanostructured Materials and Nanotechnology Division, Central Metallurgical Research and Development Institute (CMRDI), P.O. Box 87, Helwan, Cairo 11421, Egypt
Full list of author information is available at the end of the article

detection and removal of Bi(III) ions utilizing mesoporous TiO_2.

Methods

Materials

The block copolymer surfactant EO_{106}-$PO_{70}EO_{106}$(F-127,EO = $-CH_2CH_2O-$,PO = $-CH_2(CH_3)CHO-$), MW (12,600 g/mol), $Ti(OC(CH_3)_3)_4$ (TBOT), HCl, CH_3OH, C_2H_5OH, CH_3COOH, and dithizone were purchased from Sigma-Aldrich (St. Louis, MO, USA).

Preparation of mesoporous TiO_2

Mesoporous TiO_2 nanocrystals were synthesized through a simple one-step sol–gel process in the presence of the F127 triblock copolymer as a structure-directing agent. To minimize possible variables, the molar ratio of each reagent in the starting solution was fixed at TiO_2/F127/C_2H_5OH/HCl/CH_3COOH = 1:0.02:50:2.25:3.75. In particular, 1.6 g of F127, 2.3 mL of CH_3COOH, and 0.74 mL of HCl were dissolved in 30 ml of ethanol and then added to 3.5 ml of TBOT [25]. The mixture was stirred vigorously for 60 min and transferred into a Petri dish. Ethanol was subsequently evaporated at 40°C, and a relative humidity of 40% for 12 h was set followed by the transfer of the sample into a 65°C oven and ageing for an additional 24 h. The as-made mesostructured hybrids were calcined at 450°C in air for 4 h at a heating rate of 1°C/min and a cooling rate of 2°C/min to remove the surfactant and to obtain the mesostructured TiO_2.

Characterization

Transmission electron microscopy (TEM) was conducted at 200 kV with a JEOL JEM-2100 F-UHR field-emission instrument (Tokyo, Japan) equipped with a Gatan GIF 2001 energy filter (Pleasanton, CA, USA) and a 1 K CCD camera in order to obtain EEL spectra. Field emission scanning electron microscope (FE-SEM) images were carried out with a FE scanning electron microanalyzer (JEOL-6300 F, 5 kV). X-ray diffraction (XRD) data were acquired on a PANalytical X' port diffractometer using $CuK\alpha_{1/2}$, $\lambda\alpha_1$ = 154.060-pm and $\lambda\alpha_2$ = 154.439-pm radiation. Raman spectroscopy was carried out using a Perkin Elmer Raman Station 400 (Waltham, MA, USA). The nitrogen adsorption and desorption isotherms were measured at 77 K using a Quantachrome Autosorb 3B after the samples were vacuum-dried at 200°C overnight. The sorption data were analyzed using the Barrett-Joyner-Halenda (BJH) model with Halsey equation [26]. Fourier transform infrared spectroscopy (FTIR) spectra were recorded with a Bruker FRA 106 spectrometer (Ettlingen, Germany) using the standard KBr pellet method. Reflectance spectrum was taken at room temperature using UV-visible spectrophotometer (lambda 950 Perkin Elmer) fitted with universal reflectance accessory in the range of 200 to 800 nm and using $BaSO_4$ as reference.

Bi(III) ion detection

The solutions of different concentrations of Bi(III) ions ranging from 0.001 to 1 ppm were prepared in a buffer solution of pH 4. The working solution of DZ was prepared by dissolving 10 mg of dithizone in 100 ml of ethanol. The buffer solution of 0.2 M KCl-HCl of pH 2, 0.1 M CH_3COOH–CH_3COONa of pH 4, sodium dihydrogen phosphate and disodium hydrogen phosphate solution of pH 7, and 0.1 M disodium hydrogen phosphate-HCl of pH 9 was used to study the effect of pH on the adsorption of the Bi(III) ions on the designed nanosensors. A series of experiments has been carried out for the different concentrations of Bi(III) ions ranging from 0.001 to 100 ppm. For the detection of the metal ions, 5 mg of mesoporous TiO_2 was constantly stirred in 20 ml of metal-ion solution of desired pH for 5 min to achieve the heterogeneous solution. One milliliter ethanolic solution of DZ was added to the above solution at room temperature with constant stirring for 1 min. The solution was then filtered using Whatmann filter. The filtrate was then analyzed for metal ion and absorbance using UV-visible spectrophotometer (lambda 950 Perkin Elmer). Bi(III) sorption took place quantitatively as indicated from the analysis of the Bi(III) ions in effluent solutions by ICP-OES. After extraction, the ultratrace concentrations of the remained ions in the test aqueous solutions were estimated by ICP-MS. Also, the TiO_2-DZ-Bi complex was analyzed by UV-visible diffuse reflectance spectra by collecting the material from Whatmann filter. Reflectance spectrum was taken at room temperature using UV-visible spectrophotometer (lambda 950 Perkin Elmer) fitted with universal reflectance accessory in the range of 200 to 800 nm.

Results and discussion

The prepared mesoporous TiO_2, TiO_2-DZ, and TiO_2-$[(DZ)_3$-Bi] have been investigated. XRD pattern reflections from anatase phases with peaks characteristic for the (101), (004), (200), (211), and (213) lattice planes evince that TiO_2 phase easily nucleates during heating and subsequently transforms into nanocrystals upon calcination at 450°C (see Additional file 1: Figure S1). Even upon the addition of DZ anchored on the mesoporous TiO_2 (Additional file 1: Figure S1, curve b) and after the $(Bi(DZ)_3)$ complex was collected onto the surface of mesoporous TiO_2, the intensity of the mean peak (101) for all the samples was similar and there is no significant change in the crystallinity of the TiO_2 anatase phases. Nitrogen adsorption isotherms of the TiO_2 mesoporous and TiO_2-DZ are investigated (see Additional file 2:

Figure S2). Typical reversible type-IV adsorption iso-therms are found for both samples. The sharpness of the inflection resulting from capillary condensation at relative pressures p/p_0 between 0.45 and 0.7 is characteristic for mesostructures. The mesoporous TiO_2 possesses high surface areas of 174 $m^2 g^{-1}$ and large pore volumes of 0.29 $cm^3 g^{-1}$ at 450°C; they are reduced to 143 $m^2 g^{-1}$ and 0.22 $cm^3 g^{-1}$, respectively, as a result of the DZ probe anchoring the pores. Also, the pore diameter is slightly decreased from 8.11 to 6.3 nm; this further confirms the DZ probe anchoring the pores.

For the first time, we have successfully designed a highly sensitive novel sensing system and preconcentrator based on mesoporous TiO_2. Small particles and large surface area of mesoporous TiO_2 play an important role in terms of accessibility and adsorption amount. These characteristic features of sensing system increase the possibility of binding events or complex formation between metal ions and sensor, as clearly shown by our results in which the TiO_2/DZ-based nanosensor shows excellent sensing performance at ultratrace level of concentrations and also the simultaneous removal of Bi(III) ions (Figure 1). The mechanism based on binding of the Bi(III) ion with organic chromospheres (DZ) in the solution phase led to color change which corresponds to the formation of complex between Bi(III) ion and DZ, and the final interaction of the formed complex with mesoporous TiO_2 led to the formation of stable TiO_2-[(DZ)$_3$-Bi] complex which can be easily separated by simple filtration, leaving behind clear transparent filtrate (Figure 1). The sensing system responds very fast regardless of Bi(III) concentration and demonstrates color change only in few seconds. Furthermore, the designed sensor completely removed the color complex without any leaching, leaving a colorless and transparent filtrate, suggesting the stable binding between the mesoporous TiO_2 and [(DZ)$_3$-Bi] complex and also the complete removal of Bi(III) ions (Figure 1).

The TEM images of the TiO_2-DZ and TiO_2-[(DZ)$_3$-Bi] samples were investigated (Figure 2). It is clearly seen that all the particles are spherical in shape with a uniform size distribution. Interestingly, there is no change in the shape and uniformity of TiO_2 after anchoring the DZ probe (TiO_2-DZ) and even TiO_2-[(DZ)$_3$-Bi] complex (Figure 2a,b). The TEM images indicated that the prepared TiO_2 was mesoporous in nature (Figure 2a,b). The
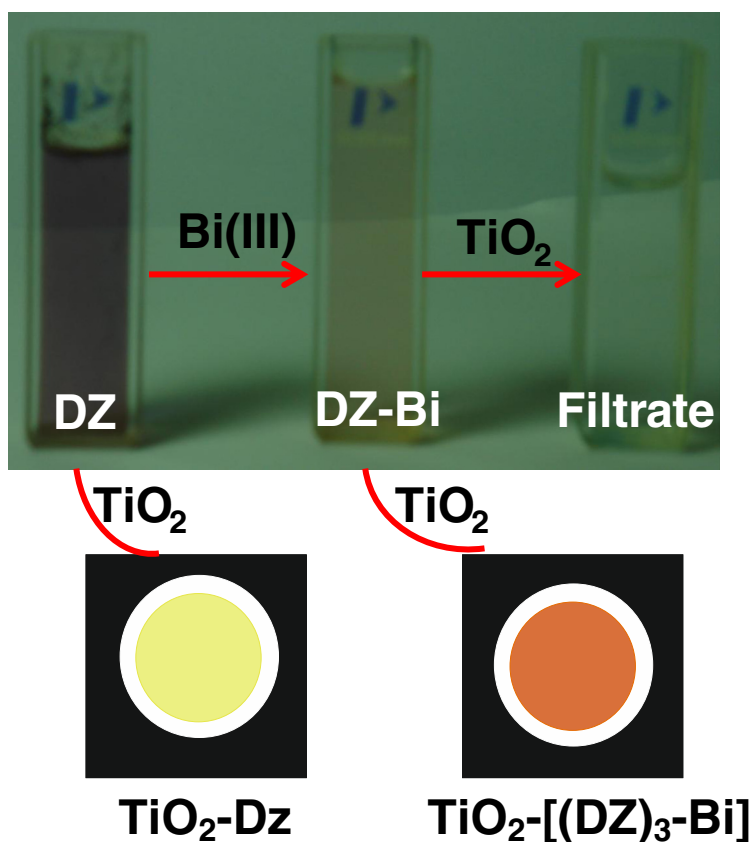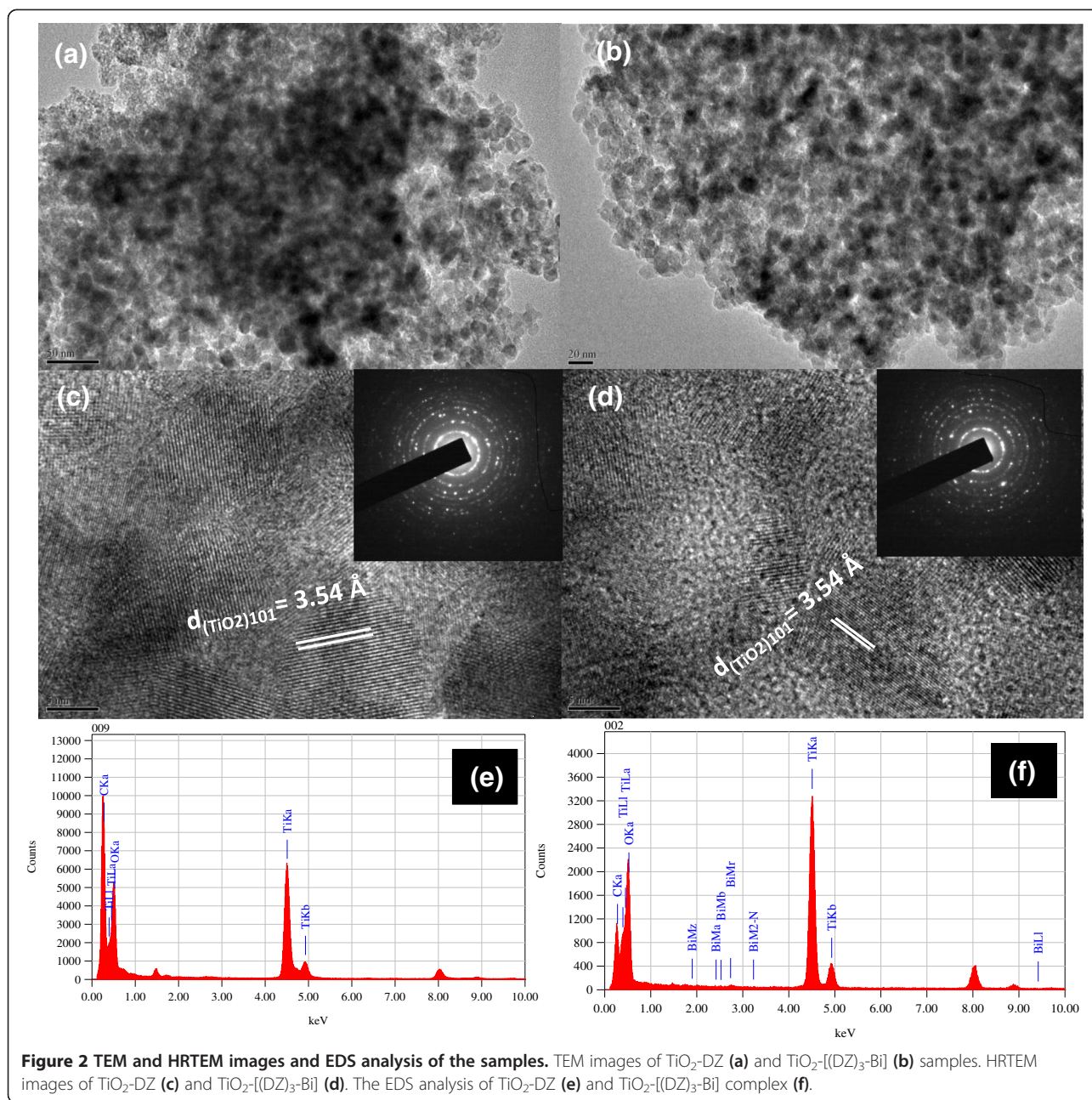

Figure 1 Sensing mechanism based on binding 0.5-ppm solution of Bi(III) ion with organic chromospheres (DZ) in solution-phase. The binding led to color change which corresponds to the formation of complex between the Bi(III) ion and DZ, and the final interaction of the formed complex with the mesoporous TiO_2 led to the formation of highly stable TiO_2-[(DZ)$_3$-Bi] complex.

Figure 2 TEM and HRTEM images and EDS analysis of the samples. TEM images of TiO_2-DZ **(a)** and TiO_2-[(DZ)$_3$-Bi] **(b)** samples. HRTEM images of TiO_2-DZ **(c)** and TiO_2-[(DZ)$_3$-Bi] **(d)**. The EDS analysis of TiO_2-DZ **(e)** and TiO_2-[(DZ)$_3$-Bi] complex **(f)**.

particle size of the TiO_2 nanocrystals has been measured to be appropriately 10 nm. As seen in the HRTEM images (Figure 2c,d), the atomic planes of the TiO_2 particles are separated by 3.54 Å, which agrees with the (101). It is important to note that the incorporation of either DZ or [(DZ)$_3$-Bi] complex into the TiO_2 framework does not have an effect on the mesostructure. The selected area electron diffraction (SAED) pattern (Figure 2c,d inset) further confirms that the TiO_2 anatase is formed. The EDS analysis showed that there is a representative EDS pattern of the TiO_2-DZ (Figure 2e) and even TiO_2-[(DZ)$_3$-Bi] complex (Figure 2f), and it revealed

the presence of Ti, O, and C elements in the obtained TiO_2-DZ; however, the Ti, O, C, and Bi elements were detected in the TiO_2-[(DZ)$_3$-Bi] sample. This indicated that the DZ probe is anchored onto the TiO_2 network, and in the case of TiO_2-[(DZ)$_3$-Bi], Bi is observed as well; this further confirms that the [(DZ)$_3$-Bi] complex was formed into the TiO_2 pores. The FTIR spectra for the meso-TiO_2, TiO_2-DZ, and TiO_2-DZ-Bi samples revealed a broad absorbance peak in the range from 3,100 to 3,450 cm^{-1} assigned to hydroxyl vibration and a strong absorbance peak around 1,628 cm^{-1} attributed to the vibrations of the surface-adsorbed H_2O and Ti-

OH bonds (see Additional file 3: Figure S3). Also, after anchoring DZ, as you see in either TiO_2-DZ or TiO_2-$[(DZ)_3$-Bi] samples, the FTIR spectra show distinct absorption peaks at 1,435 cm^{-1} corresponding to the C = S stretching mode, while the peak shifts to 1,352 cm^{-1} for the TiO_2-$[(DZ)_3$-Bi] sample due to the introduction of Bi(III) in C = S-Bi [27]. In the TiO_2-DZ and TiO_2-$[(DZ)_3$-Bi] samples, the absorption peaks at 1,540 cm^{-1} is attributed to the benzene ring stretching band, whereas in the spectrum of TiO_2-$[(DZ)_3$-Bi], the peaks shift to 1,523 cm^{-1} due to the formation of Bi-N bond in Bi-N-C_6H_5.

For the detection of Bi(III) ions, 5 mg of mesoporous TiO_2 was constantly stirred in 20 ml of Bi(III) ion solution at different concentrations and pH value of 4 for 5 min to achieve the heterogeneous solution. One milliliter ethanolic solution of DZ was added to the above solution at room temperature, and the mixture was left to allow reaction for 1 min. Change in color can be easily distinguished by naked eye, and optical changes can be easily quantified by UV-visible spectroscopy. Wide range of Bi(III) ion concentrations (0.001 to 1 ppm) has been studied using UV spectroscopy. The designed nanosensor shows high sensing ability at trace-level concentration of Bi(III) ion, suggesting easier flow of Bi(III) ion over a wide range of concentrations (Figure 3a). Mesoporous TiO_2-based sensing system can be utilized in two

ways, as a chemosensor simply by visual inspection and simultaneously this potentially interesting material could also serve as preconcentrators to provide high adsorption efficiency to remove the toxic metal ions in a single step by a strong interaction between the TiO_2 and the $[(DZ)_3$-Bi] complex. Our designed sensor provides a simultaneous detection and removal of Bi(III) ions without the use of sophisticated instrument. The stability of the DZ probe with TiO_2 can be assessed by the fact that there was no indication of elution of the probe molecules during the detection of Bi(III) ion. Transparent, clear filtrate obtained after filtration confirmed the firm integration of mesoporous TiO_2 and $Bi(DZ)_3$ complex and also the preconcentrator properties of the designed sensing system. Besides that, the addition of Bi(III) ion which led to a rapid color transformation provides a very simple, sensitive and selective detecting approach. As can be seen from Figure 3a, in the absence of Bi(III) ions, the color of the designed sensor is light yellow or mud but after the formation of the $[Bi(DZ)_3]$ complex, the color becomes light orange (at 0.001 ppm of Bi), indicating the presence of Bi in the formed complex at very low concentration of the Bi(III) ions. As the concentration of the Bi(III) ions increases, the intensity of the color also increases and becomes brick color at high concentration of the Bi(III) ions. The rapid color changing behavior of the newly developed sensing system
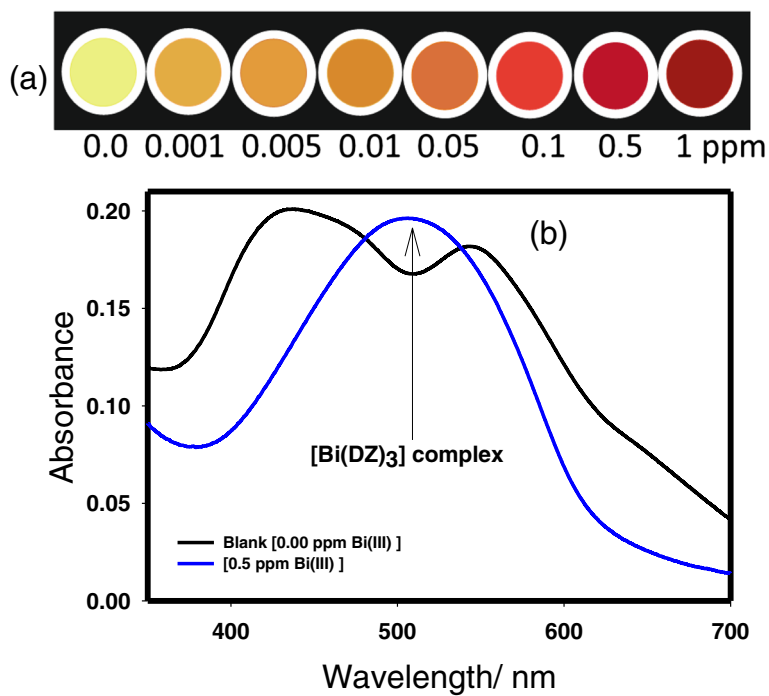

Figure 3 Color changes and spectral patterns. (a) The sequence of concentration-dependent changes in color of TiO_2-DZ nanosensor after the detection of Bi(III) ions at different concentrations. **(b)** Spectral patterns obtained with DZ in the absence (blank) and in the presence of 0.5 ppm Bi(III) ions after 1-min reaction time at pH 4.

Table 1 Absorbance values at 502 nm for each concentration studied

No.	Concentration of Bi(III) ions in ppm	Absorbance (a.u.)
1	0.001	0.1735
2	0.005	0.1771
3	0.01	0.1842
4	0.05	0.188
5	0.1	0.1936
6	0.5	0.197
7	1.0	0.217

upon the addition of the Bi(III) ions may be due the fact that highly potent mesoporous TiO_2 architecture provides proficient channeling or movement of the Bi(III) ions for efficient binding of metal ion, and the simultaneous excellent adsorbing nature of the mesoporous TiO_2 provides an extra plane for the removal of metal ions. Figure 3b shows the spectral patterns obtained with DZ-based sensor in the absence (blank) and in the presence of 0.5 ppm Bi(III) ions. As can be seen, in the absence of the Bi(III) ions, i.e., blank which shows an absorbance maxima at 434 and 580 nm. The shorter wavelength corresponds to thiol, and the longer wavelength corresponds to the thione group of DZ. On the other hand, with 0.5-ppm Bi(III) ion solution, a complex formation occurs, and a single band appears near to 502 nm which confirms the formation of the $[Bi(DZ)_3]$ complex [18-21]. The absorbance at 502 nm was used to calculate the concentration of the $[Bi(DZ)_3]$ complex. Table 1 shows the absorbance value at 502 nm for each concentration studied.

One of the major advantages of the current proposed sensing system is the selective sensing performance in the presence of interfering cations and anions even at 5,000-times-more concentration of the interfering components in comparison to Bi(III) ions (see Additional file 4: Table S1). Thus, the current approach presents a highly selective nanosensor for the efficient recognition of Bi(III) ions. To study the interfering effect of possible cations and anions which may present with Bi(III) ions in the surrounding environment or wastewater, we added the interfering cations and anions to a 0.5-ppm solution of Bi(III) ions in the presence of the proposed nanosensor at pH 4. To ensure the selective performance of our TiO_2-based sensor, we carried out the experiments up to high tolerance concentration of interfering cations and anions. The results show no significant changes at very high concentrations in color pattern obtained after the addition of various types of interfering cations and anions, confirming the highly selective nature of this mesoporous TiO_2-based sensor. Only Fe^{+3}, Cr^{+3}, and Hg^+ cations show interfering effect at high

concentrations, i.e., 100 ppm or above out of the several cations taken into consideration. In case of anions only, I^- shows slight color change at 250 ppm which is almost 5,000 times more than the Bi(III) ion concentration.

Conclusions

In summary, a very simple sensing approach for one-step detection and collection of Bi(III) ions without the use of any sophisticated technique or further modification of mesoporous TiO_2-based nanosensor is demonstrated, and the sensing results could be easily detected by naked eye. The detection limit for the Bi(III) ions using mesoporous TiO_2-based sensor is estimated to be approximately 1 ppb. The results presented herein have important implications in the development of colorimetric sensors based on mesoporous TiO_2 nanocrystals for the simple, swift, and selective detection of toxic metal ions in solution.

Additional files

Additional file 1: XRD patterns of the samples.

Additional file 2: N_2 sorption isotherms and pore size distributions (inset) of the of the samples.

Additional file 3: FTIR spectra for all the samples.

Additional file 4: Contains a table that summarizes the color trend obtained for various interfering cations and anions.

Author details
[1]Promising Centre for Sensors and Electronic Devices (PCSED), Advanced Materials and Nano-Research Centre, Najran University, P.O. Box 1988, Najran 11001, Saudi Arabia. [2]Nanostructured Materials and Nanotechnology Division, Central Metallurgical Research and Development Institute (CMRDI), P.O. Box 87, Helwan, Cairo 11421, Egypt. [3]College of Science and Arts-Sharoura, Najran University, Sharoura, Saudi Arabia. [4]Department of Physics, College of Science and Arts, Najran University, P.O. Box 1988, Najran 11001, Saudi Arabia.

References
1. Taher MA, Rezaeipor E, Afzali D: **Anodic stripping voltammetric determination of bismuth after solid-phase extraction using amberlite XAD-2 resin modified with 2-(5-bromo-2-pyridylazo)-5-diethylaminophenol.** *Talanta* 2004, **63**:797.
2. Manadal B, Ghosh N: **Combined cation-exchange and extraction chromatographic method of preconcentration and concomitant**

separation of bismuth(III) with high molecular mass liquid cation exchanger. *J Hazard Mater* 2010, **182**:363.

3. Tarigh GD, Shemirani F: **Magnetic multi-wall carbon nanotube nanocomposite as an adsorbent for preconcentration and determination of lead (II) and manganese (II) in various matrices.** *Talanta* 2013, **115**:744–750.

4. Didi MA, Sekkal AR, Villemin D: **Cloud-point extraction of bismuth (III) with nonionic surfactants in aqueous solutions.** *Colloids Surf, A* 2011, **375**:169.

5. Sun J, Chen Z, Ge M, Xu L, Zhai M: **Selective adsorption of Hg(II) by radiation synthesized silica-graft-vinyl imidazole adsorbent.** *J Hazard Mater* 2013, **244–245**:94.

6. Brown J, Richer R, Mercier L: **One-step synthesis of high capacity mesoporous Hg^{2+} adsorbents by non-ionic surfactant assembly.** *Micropor Mesopor Mater* 2000, **37**:41.

7. Idris SA, Harvey SR, Gibson LT: **Selective extraction of mercury(II) from water samples using mercapto functionalised-MCM-41 and regeneration of the sorbent using microwave digestion.** *J Hazard Mater* 2011, **193**:171.

8. Phothitontimongkol T, Siebers N, Sukpirom N, Uno F: **Preparation and characterization of novel organo-clay minerals for Hg(II) ions adsorption from aqueous solution.** *Appl Clay Sci* 2009, **43**:343.

9. Vieira RS, Beppu MM: **Dynamic and static adsorption and desorption of Hg(II) ions on chitosan membranes and spheres.** *Water Res* 2006, **40**:1726–1734.

10. Pan JY, Wang S, Zhang RF: **Preparation and modification of macroporous epoxy-triethylenetetramine resin for preconcentration and removal of Hg(II) in aqueous solution.** *J Appl Polym Sci* 2006, **102**:2372.

11. Hosseini-Bandegharaei A, Hosseini MS, Jalalabadi Y, Sarwghadi M, Nedaie M, Taherian A, Ghaznavi A, Eftekhari A: **Removal of Hg(II) from aqueous solutions using a novel impregnated resin containing 1-(2-thiazolylazo)-2-naphthol (TAN).** *Chem Eng J* 2011, **168**:1163–1173.

12. Zhu JZ, Yang J, Deng BL: **Enhanced mercury ion adsorption by amine-modified activated carbon.** *J Hazard Mater* 2009, **166**:866.

13. Zhang FS, Nriagu JO, Itoh H: **Mercury removal from water using activated carbons derived from organic sewage sludge.** *Water Res* 2005, **39**:389.

14. Ismail AA: **A selective optical sensor for antimony based on hexagonal mesoporous structures.** *J Colloid Interface Sci* 2008, **317**:288.

15. El-Safty SA, Shenashen MA, Ismail AA: **A multi-pH-dependent, single optical mesosensor/captor design for toxic metals.** *Chem Commun* 2012, **48**:9652.

16. El-Safty SA, Ismail AA, Shahat A: **Optical supermicrosensor responses for simple recognition and sensitive removal of Cu (II) ion target.** *Talanta* 2011, **83**:1341.

17. El-Safty SA, Ismail AA, Matsunaga H, Mizukami F: **Nanoscale pool-on-surface design for control sensing recognition of multiple cations.** *Adv Funct Mater* 2008, **18**:1485.

18. El-Safty SA, Ismail AA, Matsunaga H, Nanjo H, Mizukami F: **Uniformly-mesocaged cubic Fd3m monoliths as modal carriers for optical chemosensors.** *J Phys Chem C* 2008, **112**:4825.

19. El-Safty SA, Prabhakaran D, Ismail AA, Matsunaga H, Mizukami F: **Three-dimensional wormhole and ordered mesostructures and their applicability as optically ion-sensitive probe templates.** *Chem Mater* 2008, **20**:2644.

20. El-Safty SA, Ismail AA, Matsunaga H, Mizukami F: **Optical nanosensor design with uniform pore geometry and large particle morphology.** *Chem Eur J* 2007, **13**:9245.

21. El-Safty SA, Prabhakaran D, Ismail AA, Matsunaga H, Mizukami F: **Nanosensor design packages: a smart and compact development for metal ions sensing responses.** *Adv Funct Mater* 2007, **17**:3731.

22. Palomares E, Vilar R, Durrant JR: **Heterogeneous colorimetric sensor for mercuric salts.** *Chem Commun* 2004, **4**:362.

23. Nazeeruddin MK, Di Censo D, Humphry-Baker R, Grätzel M: **Highly selective and reversible optical, colorimetric, and electrochemical detection of mercury (II) by amphiphilic ruthenium complexes anchored onto mesoporous oxide films.** *Adv Funct Mater* 2006, **16**:189.

24. Sahu M, Biswas P: **Single-step processing of copper-doped titania nanomaterials in a flame aerosol reactor.** *Nanoscale Res Lett* 2011, **6**:441.

25. Fan J, Boettcher SW, Stucky GD: **Nanoparticle assembly of ordered multicomponent mesostructured metal oxides via a versatile sol–gel process.** *Chem Mater* 2006, **18**:6391.

26. Gregg SJ, Sing KSW: *Adsorption, Surface Area and Porosity.* London: Academic; 1982.

27. Zhou J, Zhao G, Yang J, Han G: **Diphenylthiocarbazone (dithizone)-assisted solvothermal synthesis and optical properties of one-dimensional CdS nanostructures.** *J Alloy Compd* 2011, **509**:6731.